NASA SP-8009

NASA SPACE VEHICLE DESIGN CRITERIA (STRUCTURES)

PROPELLANT SLOSH LOADS

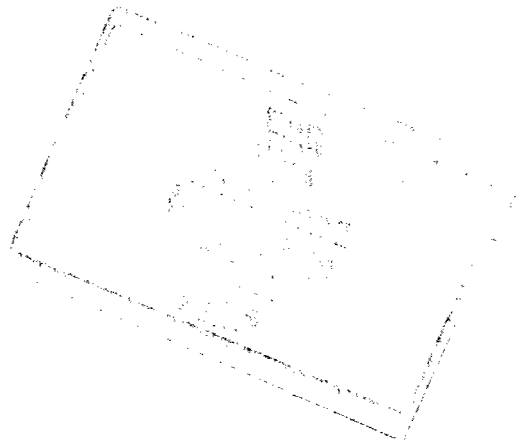

AUGUST 1968

NATIONAL AERONAUTICS AND SPACE ADMINISTRATION

FOREWORD

NASA experience has indicated a need for uniform criteria for the design of space vehicles. Accordingly, criteria are being developed in the following areas of technology:

Environment

Structures

Guidance and Control

Chemical Propulsion.

Individual components of this work will be issued as separate monographs as soon as they are completed. A list of all previously issued monographs in this series can be found on the last page of this document.

These monographs are to be regarded as guides to design and not as NASA requirements, except as may be specified in formal project specifications. It is expected, however, that the criteria sections of these documents, revised as experience may indicate to be desirable, eventually will become uniform design requirements for NASA space vehicles.

This monograph was prepared under the cognizance of the Langley Research Center. The Task Manager was A. L. Braslow. A number of individuals assisted in developing the material and in writing and reviewing the drafts. In particular, the significant contributions made by P. G. Bhuta and R. E. Hutton of TRW Systems, H. N. Abramson of Southwest Research Institute, and D. G. Stephens of NASA Langley Research Center are hereby acknowledged.

Comments concerning the technical content of these monographs will be welcomed by the National Aeronautics and Space Administration, Office of Advanced Research and Technology (Code RVA), Washington, D.C. 20546.

AUGUST 1968

For sale by the Clearinghouse for Federal Scientific and Technical Information
Springfield, Virginia 22151 – CFSTI price $3.00

CONTENTS

SYMBOLS

Symbols used in this document are defined as follows:

a	cylindrical tank radius; ellipsoidal tank minor semiaxis
a_0	inner radius of ring damper
B	similarity parameter, $\nu^{-1}\sqrt{ga^3}$
b	inner radius of circular ring tank; ellipsoidal tank major semiaxis
c_c	critical viscous damping coefficient
c_n	viscous damping coefficient
D	cylinder diameter or plate width
g	longitudinal acceleration field
h	height of quiescent fluid surface
h_0, h_1	location of rigid and first-mode sloshing masses below quiescent fluid surface
Δh	location of ring damper below quiescent fluid surface
J_0, J_1	Bessel function of the first kind and orders 0 and 1, respectively
K	nondimensional parameter in equation (10), $p/\rho U_m^2$
k	sloshing mass spring constant
ℓ	pendulum length
m	total fluid mass
m_0	nonsloshing or fixed mass
p	fluid pressure
p_0	tank pressurization
r	radial tank coordinate
T	oscillatory flow period, $2\pi/\omega$
t	time
U	oscillatory fluid flow velocity
U_m	peak oscillatory fluid flow velocity across the baffle
u_r, u_θ	radial and tangential fluid-velocity components
W	baffle width

z	distance from quiescent fluid surface to any arbitrary depth (positive direction is downward into fluid)
δ	logarithmic decrement, $2\pi\zeta<<1$
ϵ	frequency parameter
ζ_n	viscous damping ratio, c_n/c_c
η	maximum sloshing wave height, measured from quiescent fluid surface at tank wall
θ	angular tank coordinate
ν	coefficient of kinematic viscosity
ρ	fluid density
ϕ	conical tank cone angle
ω	sloshing frequency

Subscript:

1	denotes first mode except on J
n	denotes any mode

PROPELLANT SLOSH LOADS

1. INTRODUCTION

Sloshing of propellants may adversely affect the stability of a space vehicle and the integrity of the tank structure. Sloshing describes the free-surface oscillations of a fluid in a partially filled tank. These oscillations result from lateral and longitudinal displacements or angular motions of the vehicle. Such displacements or motions can be caused by several factors, alone or in combination.

Examples:

- Wind gusts during powered flight
- Programmed changes in vehicle attitude
- Attitude-stabilization control pulses
- Separation impulses
- Elastic deformations of the vehicle.

Once propellant sloshing begins, it is maintained by the continued tank motions; or in the absence of tank disturbances, the interchange of kinetic energy and the potential energies due to gravitational and surface tension forces will cause free vibrations to persist. Since the damping provided by the wiping action of the fluid against the tank walls is small, free oscillations may persist for long periods, and forced oscillations may produce large free-surface waves unless suitable damping devices are provided.

The magnitude of propellant sloshing and hence of forces and moments acting on the vehicle depends upon these parameters:

- Tank geometry
- Propellant properties
- Effective damping
- Height of propellant in the tank
- Acceleration field
- Perturbing motion of the tank.

This undesirable sloshing phenomenon may be controlled by the proper geometrical design of the tank and by the addition of baffles. Tank geometry influences the natural sloshing frequencies and sloshing modes, forced response, and resultant pressure forces and moments acting on the tank. Baffles increase the effective fluid damping and thereby reduce the duration of free oscillations and the magnitude of forced oscillations.

The spacing and configuration of baffles are determined primarily by the damping requirements. The structural strength of the baffles is determined after consideration of many factors such as the strength and rigidity needed during manufacturing and handling, the forces and thermal stresses introduced during propellant loading, and the loads due to propellant sloshing.

Dynamic coupling between the sloshing propellant and the elastic structure may have a large influence on the vibration frequencies and mode shapes of the elastic tank. This coupled propellant/elastic-tank system may also exhibit dynamic instabilities, either as an independent system or coupled with some other system component (e.g., with the combustion and feed-line systems, as in POGO).

This monograph is concerned primarily with the loads on the tank during lateral and longitudinal sloshing and with baffle pressure loads due to sloshing.

2. STATE OF THE ART

Reference 1 summarizes the development of the theory of motion of liquids and the results of various investigations of nonviscous and viscous sloshing in stationary and moving containers; reference 2 reviews various sloshing problems and investigations associated with liquid-propellant vehicles; and reference 3 is a comprehensive treatise on virtually all aspects of liquid dynamic behavior in moving containers.

2.1 Slosh Frequency and Mechanical Models

Airplane stability studies showed that the dynamic response of the vehicle to liquid sloshing could be calculated if an equivalent mechanical system were used to represent the liquid dynamics. Such mechanical systems are composed of fixed masses and oscillating masses connected to the tank by springs and dashpots or pendulums and dashpots; they have been derived for several common tank geometries (refs. 3 to 12). They are designed so that they have the same resultant pressure force, moment, damping, and frequency as the actual system. When this kind of equivalent system is combined with similar representations for other dynamic elements of the vehicle, the dynamics can be readily studied on digital and analog computers.

Reference 8 points out that increasing the size of space vehicles causes the propellant forces to be larger and to occur at lower sloshing frequencies, possibly making the stability problems more critical. However, the sloshing masses can be reduced and the frequencies can be raised by subdividing the larger tanks. Reference 8 presents the parameters for the mechanical model and calculates the sloshing forces and moments for cylindrical tanks which are separated into quarter tanks by radial dividers or into concentric cylinders by circular dividers. For a cylindrical tank, the second-mode sloshing mass is only about 3 percent of the first-mode sloshing mass; therefore, the second and higher mode sloshing effects are generally negligible. However, for the quarter tank, the second-mode sloshing mass is 43 percent of the first-mode sloshing mass and should be included in determination of the total sloshing loads acting on the tank. References 3, 5, and 13 to 15 describe procedures for determining the natural sloshing frequencies, mode shapes, and equivalent mechanical systems for sloshing in arbitrary tanks of revolution.

References 3, 6, 11, 12, and 16 to 22 report verification of predicted sloshing frequencies and demonstrate the validity of the equivalent mechanical models for rigid tanks. References 16 and 19 also show that predictions for the sloshing frequency of circular cylindrical tanks can be used to estimate the natural sloshing frequency of tanks of many other shapes, filled to various heights. In such cases, generally, the radius is taken to be that measured at the quiescent fluid surface of the actual tank, and the height of the fluid is selected to give the same volume of fluid as that in the actual tank.

For lateral sloshing in a rigid cylindrical tank with a flat bottom, the frequency in rad/sec of free-surface motion is given in reference 3 as

$$\omega_n = \sqrt{\epsilon_n \, g a^{-1} \tanh (\epsilon_n \, h a^{-1})} \qquad (1)$$

where

g longitudinal acceleration, ft/sec^2

ϵ_n determined from the root of $\left. \frac{d}{dx} J_1 (x) \right|_{x = \epsilon_n} = 0$

J_1 Bessel function of first kind and order

a tank radius, ft

h height of quiescent fluid surface, ft

Values of ϵ_n for the first four slosh modes are given in the following tabulation:

SLOSH MODE (n)	ϵ_n
1	1.841
2	5.331
3	8.536
4	11.706

For liquid heights greater than the radius of the tank, the frequency given by equation (1) may be approximated as

$$\omega_n \approx \sqrt{\epsilon_n \, ga^{-1}} \tag{2}$$

The details of the derivation and the mode shapes are given in reference 23. Tabulated data and formulas for both free and forced oscillations are given in reference 3 for many different tank configurations.

2.2 Damping

2.2.1 Smooth-Wall Damping

The magnitude of liquid damping in smooth-wall tanks has been determined for several configurations. Generally, the damping provided by the wiping action of the liquid against the walls is not adequate, and hence baffles must be added to provide the damping required to prevent instabilities in the closed-loop control system.

Measurements of damping in cylindrical, spherical, and oblate spheroidal tanks are given in references 24 to 27, and additional information is summarized in reference 3. Empirical formulas for damping in various unbaffled tanks have been derived by several investigators (ref. 3). For example, damping in unbaffled cylindrical and spherical tanks was found to correlate with the similarity parameter $B = \nu^{-1}\sqrt{ga^3}$, where g is the acceleration along the axis; a, the tank radius; and ν, the coefficient of kinematic viscosity. This parameter is derived in reference 24 from considerations of the Navier-Stokes equations. Reference 6 states that when two geometrically similar unbaffled tanks are subjected to similar sloshing, the same damping results if B is the same in both cases. The logarithmic damping δ in a circular cylindrical tank (ref. 24) can be approximated by

$$\delta = 4.98\,\nu^{\frac{1}{2}}\,a^{-\frac{3}{4}}\,g^{-\frac{1}{4}} = \frac{4.98}{\sqrt{B}}, \text{ for } \frac{h}{a} > 1 \tag{3a}$$

For a half-full spherical tank (ref. 25)

$$\delta = 0.131 \left(\frac{10^4}{2\sqrt{2}\,B} \right)^{0.359} \quad , \text{for } \frac{h}{a} = 1 \tag{3b}$$

Other empirical formulas and data for spheroidal, conical, and toroidal tanks are given in reference 3.

2.2.2 Baffle Damping

Numerous experimental and theoretical investigations have been conducted to determine the amount of effective damping provided by various baffle systems. References 3, 21, 22, 26, and 28 to 38 provide some examples. In reference 29 Miles derives a semiempirical formula for estimating the damping provided by a ring baffle in a circular cylindrical tank. This formula makes use of the experimental data obtained in reference 30. Experimental verifications of Miles' formula, together with data on its limitations for shallow fluid depths, are given in reference 31.

Baffle configurations in cylindrical tanks studied in the experiments reported in reference 32 include fixed rings, rings with radial clearance, cruciforms, and conic sections. The conic sections include upright, inverted, and perforated configurations. Further detailed information on fixed-ring baffles, and especially on the effects of perforation, is given in reference 31. Other baffle-damping investigations have studied spherical tanks (refs. 21 and 33) and oblate and prolate spheroidal tanks (refs. 22 and 26); reference 36 gives measurements of two-dimensional damping effectiveness that were used to predict the damping provided by ring baffles in cylindrical tanks.

The effects of baffle flexibility upon the damping capability of ring baffles have been studied by several investigators. The preliminary investigations of flexible baffles in reference 32 indicate that these baffles may provide more damping than rigid baffles, and further data are given in reference 35. However, the data of reference 38 indicate that flexible baffles provide increased damping only under certain conditions.

In nearly all experimental investigations of baffles, the emphasis is on the damping force (the component of the baffle force that opposes the fluid velocity) rather than on the total baffle force. However, designers of baffle systems must also know the total force acting on the baffle so they can ensure its structural adequacy. Reference 30 presents both types of baffle-force data: the total baffle force and a breakdown of it into an effective inertia force and a damping force. In the experiments reported there, the forces on cylinders and plates in oscillating flow were measured. The data indicate that these forces depend almost exclusively on the nondimensional parameter $U_m T/D$,

where the flow velocity is $U = U_m \cos \omega t$, $T = 2\pi\omega^{-1}$, D is the cylinder diameter or the plate width, ω is the sloshing frequency, and t is time. Good agreement between calculated forces and pressures on ring baffles (ref. 39) and measured values is shown in references 22 and 40.

2.3 Sloshing in Low-Gravity Fields

Propellant sloshing in fields of very low gravity has been studied by many investigators during recent years (ref. 3). Sloshing loads under low gravity are small compared with the structural capability of the tank and are probably important only as they affect control stability.

Low-gravity sloshing is characterized by the relative importance of the surface-tension forces, the contact angle, and the curved free surface of the propellant. Whether the acceleration field is low enough to require consideration of the effects of these parameters can be determined by using the Bond number—the ratio of the gravitational forces to the propellant surface-tension forces. While there is no sharply defined line of demarkation, Bond numbers much larger than unity indicate that gravity forces dominate and Bond numbers much less than unity indicate that surface-tension forces dominate. In actuality, only for Bond numbers very much larger than unity can one neglect surface-tension effects; therefore, Bond numbers as low as 100 would indicate that low-gravity effects *may* be of some significance, and Bond numbers as low as 10 would *require* consideration of low-gravity effects. Reference 3 discusses this subject and gives a variational formulation for the determination of sloshing frequencies, mode shapes, and propellant pressures under weak-gravity conditions.

An equivalent mechanical model for the representation of propellant sloshing in tanks in a weightless or near-weightless condition has recently been developed (ref. 12). The model is formed from an analysis strictly valid for Bond numbers larger than about 10; the fundamental sloshing mass and the natural frequency (for a fluid having a zero-degree contact angle) are smaller than for the usual high-g sloshing. For Bond numbers less than 10, these parameters are larger than in the high-g case. Calculated values of slosh forces and frequencies are in good agreement with experimental data measured from small models for Bond numbers between 10 and 200.

2.4 Slosh Loads

The lateral sloshing of liquid propellant in a tank results in a distributed pressure loading on the walls. The distributed pressure loading is of importance for detailed structural design. In addition, the resultant force and moment produced by the

distributed pressure are of direct importance to the design of control systems. Hence, there is considerable emphasis on equivalent mechanical models that can represent such total force and moment loads on rigid tanks.

Theoretical analyses that yield slosh forces and moments and/or pressures are available for many different tank geometries. For example, see references 5, 7, 9, and 18; other results are summarized in reference 3.

Measurements made on laboratory models have confirmed the calculated force and moment response characteristics. See, e.g., references 18, 21, 22, 28, and 41; other data are summarized in reference 3. Many of these references also contain data on slosh forces in tanks with baffles. One series of measurements of wall-pressure distributions was reported in reference 41; the total force and moment obtained by integration of the pressures, and the pressure distributions themselves, were all shown to be in good agreement with calculated values.

Recent data on the response of an elastic model of the S-IC LO_2 tank to liquid sloshing (ref. 42) indicate that equivalent mechanical model representations for rigid tanks yield the correct location for sloshing mass. The maximum measured wall displacement in the elastic model agrees with the location of the sloshing mass. However, while elastic deformations of tank walls have little effect on the propellant slosh characteristics, the converse effect of the sloshing liquid on the coupled bending frequencies of the elastic system should not be passed over lightly in the design of propellant tanks and supports. The fundamental aspects of the coupling of propellant sloshing and tank bending are well established and are summarized in reference 3.

Something should also be said about fluid pressures arising from longitudinal oscillations (ref. 3). The loads themselves are of little consequence; however, the propellant longitudinal pressure modes may couple with the elastic shell and/or the feedline and combustion system, thereby leading to vehicle dynamic instabilities such as POGO that may be serious.

2.5 Dome Impact

Propellant loading on tank domes (top or bottom) can occur for several different circumstances associated with a sudden change in the net axial acceleration: abort just following launch, boost-engine cutoff, engine start in orbit or coast flight, etc. References 3, 43, and 44 discuss various aspects of the dome-impact problem. There is no acceptable analytical or empirical procedure to evaluate these dome-impact loads; the test data cited in these references indicate that the maximum transient force on the

tank dome, as well as the pressure distribution, is quite sensitive to the test conditions and tank geometry.

3. CRITERIA

3.1 General

The structural design of propellant tanks and antislosh baffle systems shall adequately account for the propellant slosh loads in combination with all other loads and inputs.

3.2 Guides for Compliance

3.2.1 Load Determination

Propellant slosh loads shall be accurately determined for individual tank and baffle elements and shall include as a minimum the effects of the physical properties of the fluid, the fluid level, and acceleration.

3.2.2 Tests

Tests shall be made when existing information is not applicable to the tank or baffle designs. Such tests shall be conducted with the degree of similitude necessary to achieve test objectives.

4. RECOMMENDED PRACTICES

4.1 Scope

This section suggests acceptable procedures for analysis of loads on a tank structure and its baffles. These procedures are based on the linear theory of sloshing in rigid tanks. Since the lowest sloshing frequency corresponds to the lateral excitation of the tank, the design considerations are generally governed by the lateral slosh. Where possible, the analytical solutions are given for cylindrical tanks to obtain an estimate of the pressures exerted by the sloshing fluid. The sloshing models given here can be used in an overall dynamic structural analysis of the vehicle.

4.2 Tank Loads Due to Lateral Sloshing

A simple estimate can be given for the fluid pressures acting on a circular cylindrical tank during sloshing in the first lateral slosh mode. The pressure exerted on the tank walls is composed of the tank pressurization p_0, the static head ρgz, and the pressure due to lateral sloshing at the lowest natural frequency. The maximum pressure occurs in the plane of oscillation and is given by

$$p_{max} = p_0 + \rho gz + \rho g\eta \frac{\cosh\left[1.841\,(h-z)\,a^{-1}\right]}{\cosh\,(1.841\;ha^{-1})} \sin \omega_1 t \qquad (4)$$

where

- ρ fluid density, slugs/ft^3
- g longitudinal acceleration field, ft/sec^2
- η maximum wave height above quiescent fluid surface at tank walls, ft
- a tank radius, ft
- h height of quiescent fluid surface, ft
- ω_1 fundamental slosh frequency, $\sqrt{1.841\ ga^{-1} \tanh 1.841\ ha^{-1}}$, rad/sec
- z distance from quiescent fluid surface to any arbitrary depth (positive direction is downward), ft

Application of equation (4) is simplified if one notes that the total acceleration experienced by a fluid particle on the free surface varies between $g - \eta\omega_1^2$ and $g + \eta\omega_1^2$ at the wall. When the sloshing amplitude becomes large enough for the total acceleration of the fluid to be zero momentarily, the sloshing wave breaks up, and turbulent splashing begins. Taking this condition as an upper limit gives $\eta = g/\omega_1^2$, and equation (4) becomes

$$p_{max} = p_0 + \rho g \left\{ z + \frac{a \cosh\left[1.841\,(h-z)\,a^{-1}\right]}{(1.841 \sinh\,(1.841\;ha^{-1})} \right\} \qquad (5)$$

When the fluid height is roughly equal to or greater than the tank radius, the dynamic behavior of the fluid becomes independent of depth and the pressure equation is approximated by

$$p_{max} = p_0 + \rho g \left[z + \frac{a}{1.841} e^{-1.841\,za^{-1}} \right] \qquad (6)$$

This pressure equation is still approximately valid even if the tank does not have a flat bottom. For lower fluid heights the equation becomes less accurate, but then the total sloshing pressures are also small. For other tank configurations, the analyses described in references such as 5, 7, 8, and 13 to 15 can be used.

In general, approximately the lower third of the fluid behaves essentially as a rigid mass, while most of the sloshing effects occur near the surface. This is the basis upon which most of the various mechanical analogies involving spring-mass or pendulum systems are founded. Integration of wall pressure distributions from bottom to surface will yield the total force and moment acting on the tank, and it is often possible to devise mechanical analogies that will represent these forces and moments quite accurately, even for tanks of rather complex geometry. However, care should be taken when applying such models to off-resonance conditions, since the fluid pressures may still be quite large even though the resultant force is very small (ref. 41).

The sloshing mass, and hence the resulting fluid force, decreases rather substantially in the higher modes of oscillation. In the lowest modes the slosh mass may be effectively reduced by subdivision of the tank into radial or concentric compartments. This subdivision also reduces the slosh forces and at the same time shifts the slosh frequencies. The total force and moment response of tanks of various geometries to excitations of several different types and orientations have been considered, and both theoretical and experimental data are available (ref. 3).

4.3 Tank Loads Due to Longitudinal Sloshing

4.3.1 Oscillating Liquid Modes

When the propellant sloshes in a longitudinal mode, the integrated pressures over the tank bottom and walls have a zero resultant pressure force. An estimate of the fluid pressure forces during fluid sloshing in the first longitudinal mode in a circular cylindrical tank at the fundamental longitudinal frequency ω_1 is given by

$$p = p_0 + \rho g \left[z + \eta \frac{J_0 (3.83\, ra^{-1})}{J_0 (3.83)} \frac{\cosh [3.83 (ha^{-1} - za^{-1})]}{\cosh (3.83\, ha^{-1})} \sin \omega_1 t \right] \quad (7)$$

For a fluid height approximately equal to or greater than the tank radius, and again assuming $\eta = g/\omega_1^2$, the maximum pressure becomes

$$p_{max} = p_0 + \rho g \left[z + \frac{a}{3.83} \frac{J_0 (3.83\ ra^{-1})}{J_0 (3.83)} e^{-3.83\, za^{-1}} \right] \tag{8}$$

The effect of elasticity of the tank bottom is to lower the natural sloshing frequencies of the fluid surface slightly below their values in a rigid tank.

The internal pressurized liquid and gas columns, together with the elastic structure, constitute a rather complex system which exhibits motions of the fluid surface, bending and breathing motions of the tank walls, breathing of the tank bottom, and pressure oscillations in the fluid column. These various kinds of response are of particular importance with respect to overall vehicle dynamic characteristics, as in the POGO problem. At present, general methods of analysis are either unavailable or unreliable so that specific vehicle problems must be individually investigated.

4.3.2 Dome Impact

The loads on a tank dome or bulkhead resulting from gross longitudinal motion of the propellant may be of concern. Fluid impact on deflector baffles may also produce significant loads. Unfortunately, there are no general methods of analysis for predicting such loads and therefore empirical calculations or tests, or both, must be used. Ring baffles and other internal hardware will significantly reduce fluid impact loads.

4.4 Mechanical Models for Lateral Sloshing

Mechanical models which simulate the resultant dynamic pressure forces and moments that act on a tank during sloshing are presented in figures 1 to 3. Table I lists the mechanical model parameters used to represent the first-mode lateral sloshing in circular cylindrical and 45° conical tanks. Other mechanical models for these tanks and for other tank geometries are discussed in detail in reference 3. A mechanical model for low-gravity sloshing in a cylindrical tank is developed in reference 12.

Table I

Basic Data and Mechanical Models for Representing First-Mode Lateral Sloshing in Circular Cylindrical and 45° Conical Tanks

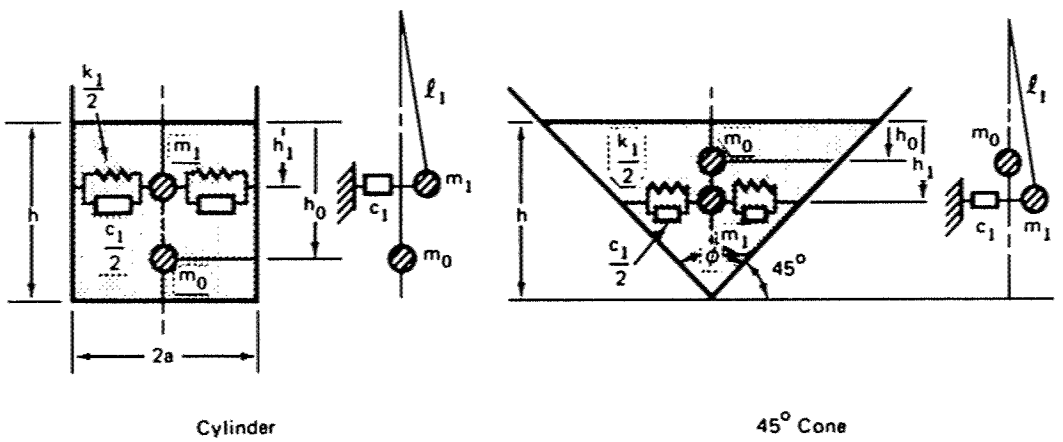

Cylinder

45° Cone

CHARACTERISTICS	CYLINDER	45° CONE
Natural frequency, ω_1	$\sqrt{1.841\ g a^{-1}\ \tanh\ (1.841\ h a^{-1})}$	$\sqrt{g h^{-1}}$
Sloshing-mass ratio, m_1/m	$0.4547\ a h^{-1}\ \tanh\ (1.841\ h a^{-1})$	0.75
Fixed-mass ratio, m_0/m	$1 - \frac{m_1}{m}$	0.25
Spring constant, k_1	$m_1 \omega_1^{\ 2}$	$m_1 \omega_1^{\ 2}$
Sloshing-mass location ratio, h_1/h	$1.08\ a h^{-1}\ \tanh\ (0.920\ h a^{-1})$	0.4
Fixed-mass location ratio, h_0/h	$\frac{1}{2}\ \frac{m}{m_0} - \left(\frac{m_1}{m_0}\right)\left(\frac{h_1}{h}\right)$	−0.2
Pendulum-length ratio, ℓ_1/h	$0.5432\ a h^{-1}\ \coth\ (1.841\ h a^{-1})$	1
Damping coefficient, c_1	$2 m_1 \omega_1 \zeta_1$	$2 m_1 \omega_1 \zeta_1$

Figure 1 shows the mechanical model parameters for first-mode sloshing in a circular cylindrical ring tank as functions of the ratio of fluid height to tank radius (h/a) for ratios of inner tank radius to outer tank radius (b/a) of 0, 0.5, and 0.9. The effective sloshing mass of the second mode is less than 3 percent that of the first mode.

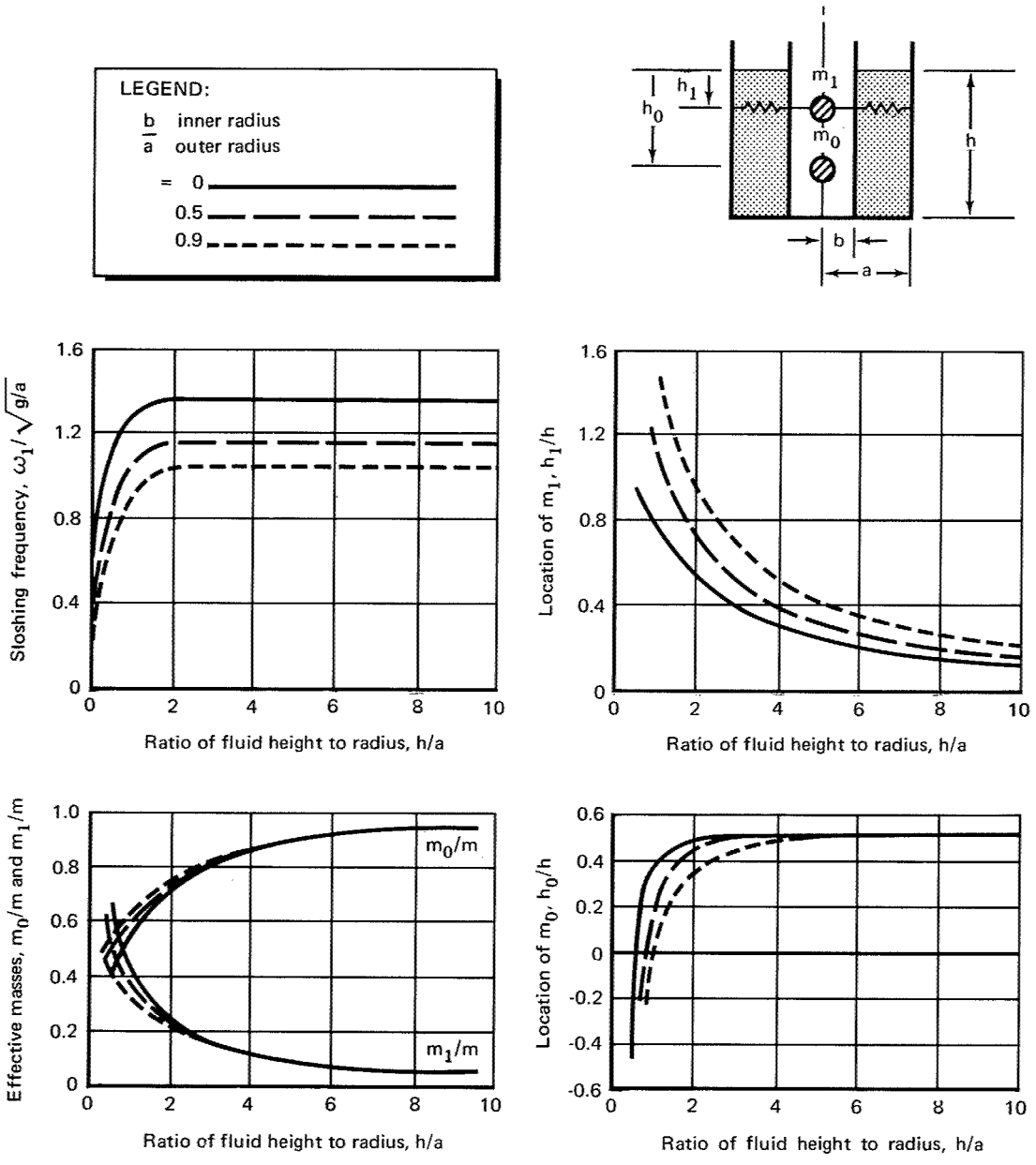

Figure 1

Frequency, effective masses, and mass attachment points for the lumped spring-mass model representation of first-mode lateral sloshing in circular cylindrical ring tanks for various ratios of inner tank radius to outer tank radius.

Figure 2 shows the mechanical model parameters for first-mode sloshing in an axisymmetric ellipsoidal tank for height-to-width ratios b/a of 2, 1 (spherical tank), and 0.5.

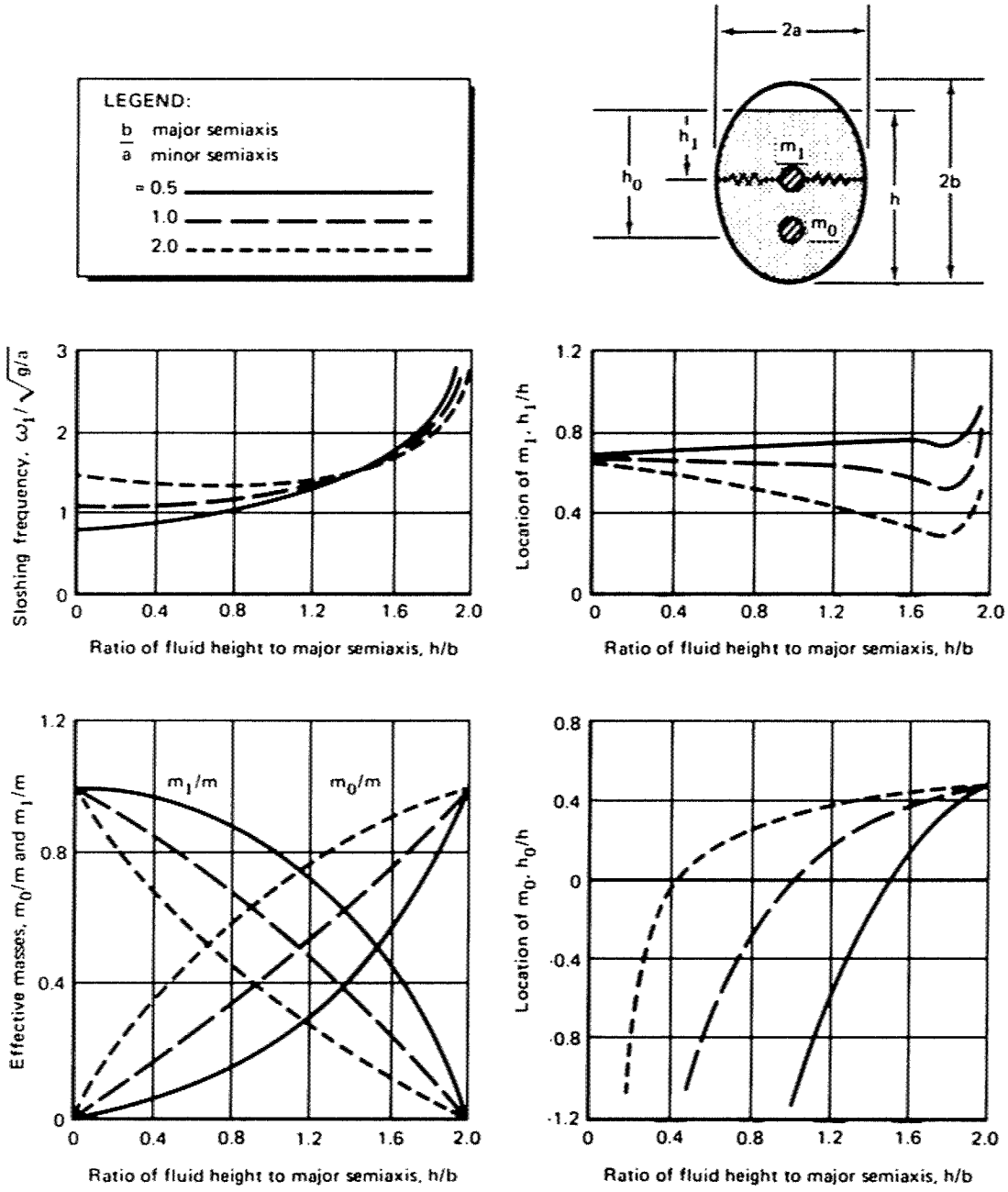

Figure 2

Frequency, effective masses, and mass attachment points for the lumped spring-mass model representation of first-mode lateral sloshing in an ellipsoidal tank.

Figure 3 shows the mechanical model parameters for first-mode sloshing in a conical tank for various cone angles ϕ.

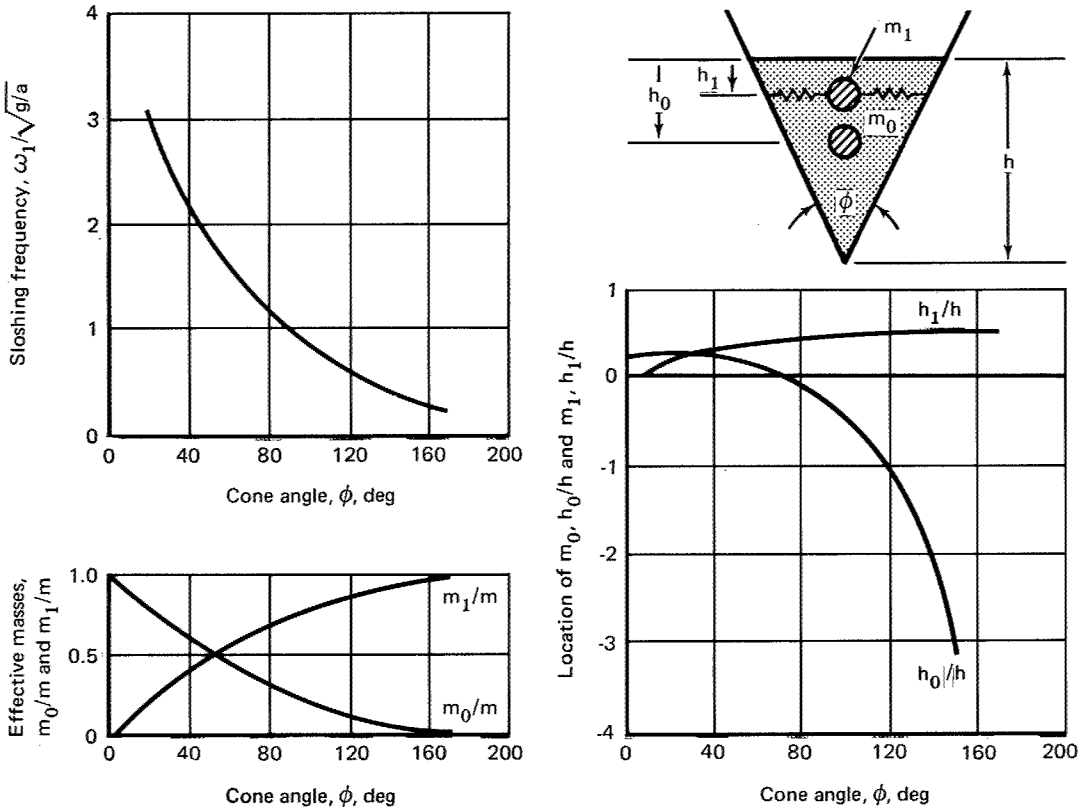

Figure 3

Frequency, effective masses, and mass attachment points for the lumped spring-mass model representation of first-mode lateral sloshing in a conical tank.

These types of mechanical analogies for slosh forces and moments in rigid tanks can often adequately represent the dynamical problem, provided (1) that multimass mechanical models be employed if the excitation frequency is expected to be close to any of the higher-order slosh modes and (2) that damping effects be considered if the range of interest is in the very near neighborhood of the fundamental slosh mode. There is no satisfactory procedure available by which the effects of tank elasticity can be introduced into such mechanical models.

The foregoing data on the parameters for mechanical models were calculated directly from analyses of sloshing force and moment. Newly developed models should be checked by experiments and, in fact, the model parameters themselves can be determined directly from such tests (refs. 11 and 34).

4.5 Baffle Damping

Slosh damping in baffled and unbaffled tanks is determined largely by experimental and semiempirical methods. An approximation for the damping ratio ζ (related to the logarithmic decrement δ by the equation $\delta = 2\pi\zeta$) due to solid ring baffles in cylindrical tanks is shown in figure 4 as an effective damping ratio. This approximation is based on the assumption that the baffle remains in the fluid during sloshing. Hence, when the baffle is near the free surface ($\Delta h/a$ less than about 0.2), the baffle will be above the fluid periodically during sloshing, and the effective damping will be somewhat less than that which may be extrapolated from figure 4. An estimate of the combined damping ratio of a series of ring baffles is generally made from figure 4 by adding the individual effect of each ring, although this method for obtaining the total effect has not been rigorously verified by either test or theory.

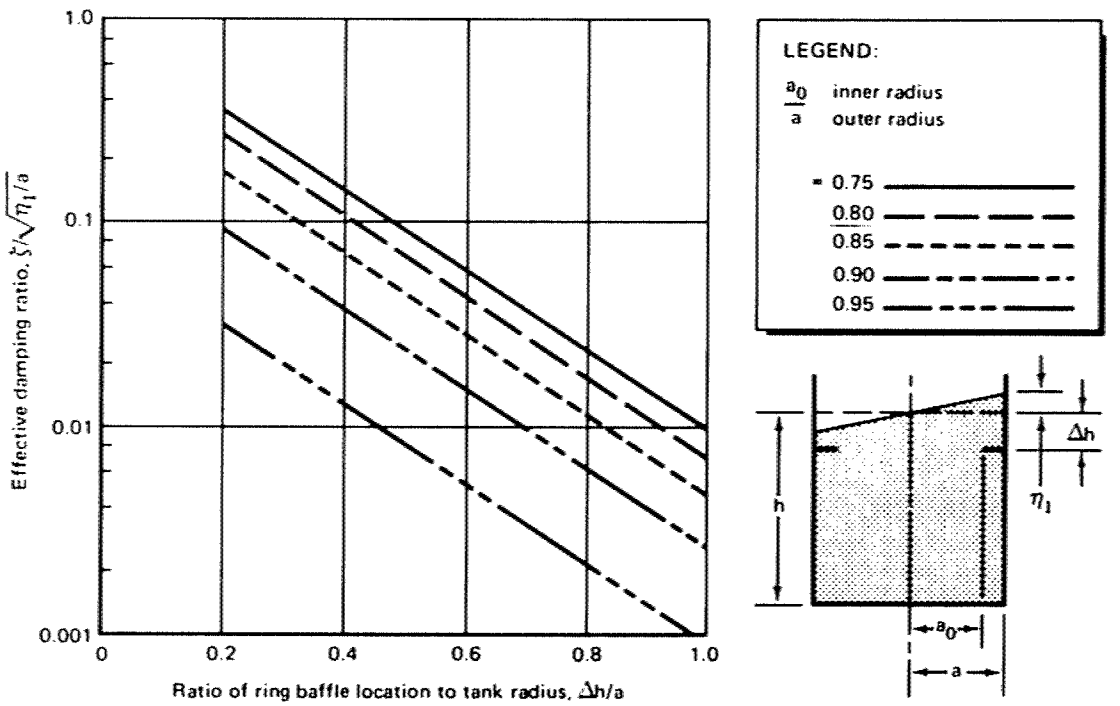

Figure 4
Estimated damping ratio for ring baffles in a circular cylindrical tank.

The damping ratio ζ can be used to compute an effective viscous damping coefficient c_1 in the mechanical models. The relation between these two coefficients, from linear theory, is

$$c_1 = 2m_1\omega_1\zeta \tag{9}$$

Additional data on damping in various kinds of tanks with various baffle systems are given in references 21, 22, 26, and 29 to 36. Note that baffles may be perforated to reduce weight, but the optimum hole size and percent perforation must be determined empirically from test data.

4.6 Baffle Pressure Loadings

4.6.1 Ring Baffles

The maximum pressure acting on a submerged baffle subjected to the oscillatory fluid-flow velocity $U = U_m \cos \omega t$ during sloshing can be computed from the equation

$$p = K\rho U_m^2 \tag{10}$$

where K is the nondimensional parameter shown in figure 5; it depends on the baffle width W, the fluid oscillatory frequency ω, and the maximum fluid velocity U_m.

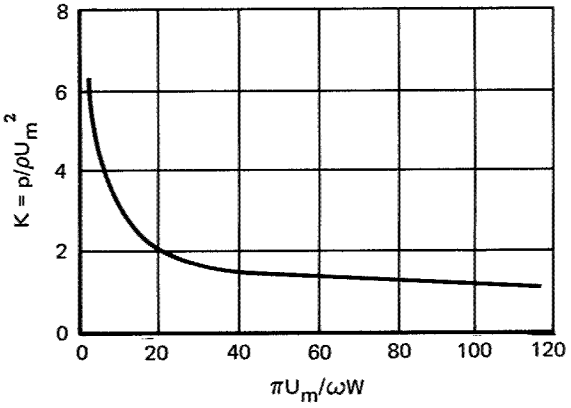

Figure 5
Nondimensional baffle pressure (from fig. 32 of ref. 30).

The maximum vertical fluid velocity at any height in a circular cylindrical tank is

$$U_m = \frac{1.841\ g}{\omega_1\ a}\ \eta\ \frac{\sinh\left[1.841\ (h-z)\ a^{-1}\right]}{\cosh\left[1.841\ ha^{-1}\right]} \tag{11}$$

where

$$\omega_1 = \sqrt{1.841\ ga^{-1}\ \tanh\left(1.841\ ha^{-1}\right)}$$

is the sloshing natural frequency in the first lateral mode. By use of these relations, and with the assumption that the fluid height is nearly equal to or greater than the tank radius, the fluid-pressure equation can be approximated by

$$p = K\rho\omega_1^2 \eta^2 e^{-3.682 Za^{-1}} \tag{12}$$

Here again, if η is taken as g/ω_1^2 , the maximum baffle pressure is approximately

$$p = \frac{K\rho ga}{1.841} e^{-3.682 Za^{-1}} \tag{13}$$

An essentially equivalent set of relations is given in reference 39, and both analyses are compared with test data in reference 40. The agreement between the test data and the two analyses is generally good, although it must be noted that the analyses are based on inviscid flow theory and hence will probably not give an accurate estimate of the occurrence of the maximum pressure on the baffle during the slosh cycle. Perforation of the baffle can reduce the force acting on the baffle by as much as 25 to 30 percent.

When the baffle is just above the quiescent fluid surface, it is periodically subjected to the slapping action of the sloshing wave. By applying impulse momentum and assuming that the velocity of the fluid is completely reversed when it strikes the baffle, one obtains the pressure equation

$$p = 2\rho U_m^2 \tag{14}$$

where U_m is the fluid velocity at impact. For $U_m = \omega_1 \eta_1$, equation (14) gives

$$p = 2\rho\omega_1^2 \eta_1^2 \tag{15}$$

If the value of η_1 is again taken as g/ω_1^2 and if $h \geqslant a$, the maximum pressure is

$$p_{max} = \frac{2\rho ga}{1.841} \tag{16}$$

4.6.2 Other Baffle Systems

Tests on baffle systems other than ring baffles have been made by several investigators (e.g., refs. 3, 30, 32, and 34). Generally, fluid sloshing loads on such baffle systems as antivortex baffles and truss-type baffles are smaller than the inertia loadings because the fluid velocities at the location of the submerged baffles are usually small. The fluid pressure loadings that do exist can be expressed by an equation of the form of equation (10), where the parameter K depends upon the baffle shape and the nondimensional parameter $U_m T/D$. Reference 30 gives data on values of K for oscillatory flow about cylinders and plates. For a steady flow that is completely reversed as it impacts on the baffle, equation (14) gives the value of K as 2. The fluid velocity U_m can be determined from the velocity potential function, which can be found for an arbitrary tank by the methods of references 3, 5, and 13. For a fluid sloshing in its first lateral mode in a circular cylindrical tank (ref. 7), the radial and tangential fluid-velocity components are

$$u_r = \frac{g\eta}{\omega_1}\left[\frac{1.841\ J_0\ (1.841\ ra^{-1})}{aJ_1\ (1.841)} - \frac{1}{r}\ \frac{J_1\ (1.841\ ra^{-1})}{J_1\ (1.841)}\right] \cos\theta\ \frac{\cosh\left[1.841\ (h-z)\ a^{-1}\right]}{\cosh\ (1.841\ ha^{-1})}\ \cos\omega_1 t \qquad (17)$$

and

$$u_\theta = -\frac{g\eta}{\omega_1}\ \frac{J_1\ (1.841\ ra^{-1})}{rJ_1\ (1.841)}\ \sin\theta\ \frac{\cosh\left[1.841\ (h-z)\ a^{-1}\right]}{\cosh\ (1.841\ ha^{-1})}\ \cos\omega_1 t \qquad (18)$$

from which the resultant fluid velocity can be calculated.

4.7 Tests

For tank or baffle designs that are very different from existing designs for which frequency, damping, and loads data are available, additional tests should be performed. Such tests can be conducted in the same way as those described in references 3, 26, 28, 30 to 38, and 40. References 3, 24, 28, and 45 discuss the model laws for sloshing of an incompressible viscous fluid having negligible surface tension in a rigid tank. These references show that the response of the prototype to a given tank motion will be dynamically similar to that of the model, provided the tanks are geometrically similar and filled to equivalent heights, and that the single nondimensional parameter $B = \nu^{-1}\sqrt{ga^3}$ is the same for the prototype as for the model. Reference 45 discusses the

general model laws when fluid compressibility, vapor pressure, tank flexibility, and other effects are important. Reference 3 discusses modeling in which surface tension forces are important; for example, fluid sloshing in a low-gravity field.

The parameters to be measured in these model tests are the sloshing natural frequencies, effective fluid damping, and forces acting on the tank and its baffle system. The test procedures for making such measurements are discussed extensively in the cited references. Tests of the type discussed in reference 3, in which a weightless or nearly weightless condition must be simulated and in which the fluid contact angle at the wall and the surface tension must be modeled, are much more difficult to perform. However, from a loads viewpoint, such tests will probably not be required.

REFERENCES

1. Cooper, R. M.: Dynamics of Liquids in Moving Containers. ARS J., vol. 30, no. 8, Aug. 1960, pp. 725-729.

2. Abramson, H. N.: The Dynamic Behavior of Liquids in Moving Containers. Applied Mechanics Review, vol. 16, no. 7, July 1963, pp. 501-506.

3. Abramson, H. N., ed.: The Dynamic Behavior of Liquids in Moving Containers. NASA SP-106, 1966.

4. Graham, E. W.; and Rodriguez, A. M.: The Characteristics of Fuel Motion Which Affect Airplane Dynamics. J. Appl. Mech., vol. 19, no. 3, Sept. 1952, pp. 381-388.

5. Lomen, D. O.: Liquid Propellant Sloshing in Mobile Tanks of Arbitrary Shape. NASA CR-222, Apr. 1965.

6. Abramson, H. N.; Chu, W. H.; and Ransleben, G. E., Jr.: Representation of Fuel Sloshing in Cylindrical Tanks by an Equivalent Mechanical Model. ARS J., vol. 31, no. 12, Dec. 1961, pp. 1697-1705.

7. Bauer, H. F.: Theory of the Fluid Oscillations in a Circular Cylindrical Ring Tank Partially Filled With Liquid. NASA TN D-557, 1960.

8. Bauer, H. F.: Fluid Oscillations in the Containers of a Space Vehicle and Their Influence Upon Stability. NASA TR R-187, 1964.

9. Rattayya, J. V.: Sloshing of Liquids in Axisymmetric Ellipsoidal Tanks. Preprint 65-114, Am. Inst. Aeron. Astronaut., Jan. 25-27, 1965.

10. Koelle, H. H., ed.: Handbook of Astronautical Engineering. McGraw-Hill Book Co., Inc., 1961.

11. Dodge, F. T.; and Kana, D. D.: Moment of Inertia and Damping of Liquids in Baffled Cylindrical Tanks. J. Spacecraft Rockets, vol. 3, no. 1, Jan. 1966, pp. 153-155.

12. Dodge, F. T.; and Garza, L. R.: Experimental and Theoretical Studies of Liquid Sloshing at Simulated Low Gravities. J. Appl. Mech., vol. 34, no. 3, Sept. 1967, pp. 555-562.

13. Lawrence, H. R.; Wang, C. J.; and Reddy, R. B.: Variational Solution of Fuel Sloshing Modes. Jet Propulsion, vol. 128, no. 11, Nov. 1958, pp. 729-736.

14. Lomen, D. O.: Digital Analysis of Liquid Propellant Sloshing in Mobile Tanks With Rotational Symmetry. NASA CR-230, May 1965.

15. Moiseev, N. N.; and Petrov, A. A.: The Calculation of Free Oscillations of a Liquid in a Motionless Container. Advances in Applied Mechanics. Vol. IX. Academic Press, Inc., 1966, pp. 91-154.

16. Abramson, H. N.; and Ransleben, G. E., Jr.: Some Comparisons of Sloshing Behavior in Cylindrical Tanks With Flat and Conical Bottoms. ARS J., vol. 31, no. 4, Apr. 1961, pp. 542-544.

17. Warner, R. W.; and Caldwell, J. T.: Experimental Evaluation of Analytical Models for the Inertias and Natural Frequencies of Fuel Sloshing in Circular Cylindrical Tanks. NASA TN D-856, 1961.

18. Stofan, A. J.; and Armstead, A. L.: Analytical and Experimental Investigation of Forces and Frequencies Resulting from Liquid Sloshing in a Spherical Tank. NASA TN D-1281, 1962.

19. Leonard, H. W.; and Walton, W. C., Jr.: An Investigation of the Natural Frequencies and Mode Shapes of Liquids in Oblate Spheroidal Tanks. NASA TN D-904, 1961.

20. Stephens, D. G.; and Leonard, H. W.: The Coupled Dynamic Response of a Tank Partially Filled with a Liquid and Undergoing Free and Forced Planar Oscillations. NASA TN D-1945, 1963.

21. Abramson, H. N.; Chu, W. H.; and Garza, L. R.: Liquid Sloshing in Spherical Tanks. AIAA, vol. 1, no. 2, Feb. 1963, pp. 384-389.

22. Kana, D. D.; Silverman, S.; Garza, L. R.; and Abramson, H. N.: Liquid Sloshing in Laterally and Longitudinally Excited Rigid Spheroids. Tech. Summary Rept., Part I. Contract NAS8-20329, Southwest Research Institute, Jan. 1967.

23. Lamb, H.: Hydrodynamics. Sixth ed., Dover Publications, 1945, pp. 284-289.

24. Berlot, R. R.; Birkhoff, G.; and Miles, J. W.: Slosh Damping in a Rigid Cylindrical Tank. Rept. GM-TR-263, Ramo-Wooldridge Corp. (now TRW, Inc.), Oct. 1957.

25. Sumner, I. E.; and Stofan, A. J.: An Experimental Investigation of the Viscous Damping of Liquid Sloshing in Spherical Tanks. NASA TN D-1991, 1963.

26. Stephens, D. G.; Leonard, H. W.; and Silveira, M. A.: An Experimental Investigation of the Damping of Liquid Oscillations in an Oblate Spheroidal Tank With and Without Baffles. NASA TN D-808, 1961.

27. Stephens, D. G.; Leonard, H. W.; and Perry, T. W., Jr.: Investigation of the Damping of Liquids in Right-Circular Cylindrical Tanks, Including the Effects of a Time-Variant Liquid Depth. NASA TN D-1367, 1962.

28. Abramson, H. N.; and Ransleben, G. E., Jr.: Simulation of Fuel Sloshing Characteristics in Missile Tanks by Use of Small Models. ARS J., vol. 30, no. 7, July 1960, pp. 603-612.

29. Miles, J. W.: Ring Damping of Free Surface Oscillations in a Circular Tank. J. Appl. Mech., vol. 25, no. 2, June 1958, pp. 274-276.

30. Keulegan, G. H.; and Carpenter, L. H.: Forces on Cylinders and Plates in an Oscillating Fluid. J. Res. Natl. Bur. Std., vol. 60, no. 5, May 1958, pp. 423-440.

31. Abramson, H. N.; and Garza, L. R.: Some Measurements of the Effects of Ring Baffles in Cylindrical Tanks. J. Spacecraft Rockets, vol. 1, no. 5, Sept.-Oct. 1964, pp. 560-562.

32. Silveira, M. A.; Stephens, D. G.; and Leonard, H. W.: An Experimental Investigation of the Damping of Liquid Oscillations in Cylindrical Tanks With Various Baffles. NASA TN D-715, 1961.

33. Sumner, I. E.: Experimental Investigation of Slosh-Suppression Effectiveness of Annular-Ring Baffles in Spherical Tanks. NASA TN D-2519, 1964.

34. Sumner, I. E.; Stofan, A. J.; and Shramo, D. J.: Experimental Sloshing Characteristics and a Mechanical Analogy of Liquid Sloshing in a Scale-Model Centaur Liquid Oxygen Tank. NASA TM X-999, 1961.

35. Stephens, D. G.; and Scholl, H. F.: Effectiveness of Flexible and Rigid Ring Baffles for Damping Liquid Oscillations in Large-Scale Cylindrical Tanks. NASA TN D-3878, 1967.

36. Cole, H. A., Jr.; and Gambucci, B. J.: Measured Two-Dimensional Damping Effectiveness of Fuel-Sloshing Baffles Applied to Ring Baffles in Cylindrical Tanks. NASA TN D-694, 1961.

37. Cole, H. A., Jr.: On a Fundamental Damping Law for Fuel Sloshing. NASA TN D-3240, 1966.

38. Garza, L. R.; and Dodge, F. T.: A Comparison of Flexible and Rigid Ring Baffles for Slosh Suppression. J. Spacecraft Rockets, vol. 6, no. 4, June 1967, pp. 805-806.

39. Liu, F. C.: Pressure on Ring Baffles Due to Fuel Sloshing in a Cylindrical Tank. Rept. R-Aero-4-64, NASA-MSFC, Jan. 1964.

40. Garza, L. R.: Theoretical and Experimental Pressures and Forces on a Ring Baffle Under Sloshing Conditions. J. Spacecraft Rockets, vol. 3, no. 2, Feb. 1966, pp. 276-278.

41. Abramson, H. N.; and Ransleben, G. E., Jr.: Wall Pressure Distributions During Sloshing in Rigid Tanks. ARS J., vol. 31, no. 4, Apr. 1961, pp. 545-547.

42. Kana, D. D.; Gormley, J. F.; Garza, L. R.; and Abramson, H. N.: Vibrational Characteristics of a Model Space Vehicle Propellant Tank. Tech. Summary Rept., Part II. Contract NAS8-20329, Southwest Research Institute, Jan. 1967.

43. Epperson, T. B.; Brown, R.; and Abramson, H. N.: Dynamic Loads Resulting From Fuel Motion in Missile Tanks. Advances in Ballistic Missile and Space Technology. Vol. II. Pergamon Press, Inc., 1961, pp. 313-327.

44. Stephens, D. G.: Experimental Investigation of Liquid Impact in a Model Propellant Tank. NASA TN D-2913, 1965.

45. Sandorff, P. E.: Principles of Design of Dynamically Similar Models for Large Propellant Tanks. NASA TN D-99, 1960.

NASA SPACE VEHICLE DESIGN CRITERIA MONOGRAPHS ISSUED TO DATE

SP-8001 (Structures)	Buffeting During Launch and Exit, May 1964
SP-8002 (Structures)	Flight-Loads Measurements During Launch and Exit, December 1964
SP-8003 (Structures)	Flutter, Buzz, and Divergence, July 1964
SP-8004 (Structures)	Panel Flutter, May 1965
SP-8005 (Environment)	Solar Electromagnetic Radiation, June 1965
SP-8006 (Structures)	Local Steady Aerodynamic Loads During Launch and Exit, May 1965
SP-8007 (Structures)	Buckling of Thin-Walled Circular Cylinders, September 1965
SP-8008 (Structures)	Prelaunch Ground Wind Loads, November 1965
SP-8010 (Environment)	Models of Mars Atmosphere (1967), May 1968

NASA-Langley, 1968 —— 32

NATIONAL AERONAUTICS AND SPACE ADMINISTRATION
WASHINGTON, D. C. 20546

OFFICIAL BUSINESS

FIRST CLASS MAIL

POSTAGE AND FEES PAID
NATIONAL AERONAUTICS AND
SPACE ADMINISTRATION

01U 003 25 21 1AS 68351 00010
NASA
MARSHALL SPACE FLIGHT CENTER
HUNTSVILLE, ALABAMA 35812

ATT LIBRARY SERVICES SECTION, CODE MS-IL

POSTMASTER: If Undeliverable (Section 158 Postal Manual) Do Not Return